https://doi.org/10.5194/se-2019-184
Preprint. Discussion started: 10 December 2019


Solid Earth
Discussions
Open Access
EGU

# A review and evaluation of the methodology for digitising 2D fracture networks and topographic lineaments in GIS

Romesh Palamakumbura[1], Maarten Krabbendam[1], Katie Whitbread[1] and Christian Arnhardt[2]

[1]British Geological Survey, The Lyell Centre, Research Avenue South, Edinburgh EH14 4AP, UK

[2]British Geological Survey, Nicker Hill, Keyworth NG12 5GG

**Abstract.** Understanding the impact of fracture networks on rock mass properties is an essential part of a wide range of fields in geosciences, from understanding permeability of groundwater aquifers and hydrocarbon reservoirs to erodibility properties and slope stability of rock masses for geotechnical engineering. However, gathering high quality, oriented-fracture datasets in the field can be difficult and time consuming, for example due to constraints on time or access (e.g. cliffs). Therefore, a method for obtaining accurate, quantitative fracture data from photographs is a significant benefit. In this paper we describe and evaluate the method for generating a series of digital fracture traces in GIS-environment, in which spatial analysis of a fracture network can be carried out. The method is not meant to replace the gathering of data in the field, but to be used in conjunction, and is well suited where fieldwork time is limited, or where the section cannot be accessed directly. The basis of the method is the generation of the vector dataset (shapefile) of a fracture network from a georeferenced photograph of an outcrop in a GIS environment. From that shapefile, key parameters such as fracture density and orientation can be calculated. Furthermore, in the GIS-environment more complex spatial calculations and graphical plots can be carried out such as heat maps of fracture density. There are a number of advantages to using a digital method for gathering fracture data including: time efficiency, generating large fracture network datasets, flexibility during data gathering and consistency of data.

## 1 Introduction

Fractures are the main pathways of fluid flow in rocks, and exert a strong influence on rock mass properties. The characterisation of fracture networks is an essential aspect of various parts of earth science, for example to understand and predict the behaviour of fluid flow in groundwater aquifers and hydrocarbon reservoirs, and the erodibility and slope stability of rock masses. Fracture network data are essential for assessing future sites of nuclear waste repositories, predicting rock slope stability and understanding intact rock strength for engineering of infrastructure (e.g. Selby, 1982; Hoek and Brown, 1997; Singhal and Gupta, 2010; Park et al., 2005; Follin et al. 2014; Zhan et al., 2017; Ren et al., 2017). For 2D fracture network analysis, there are a number fracture parameters that are widely used, including orientation, spacing, length, density/intensity and various connectivity proxies (summarised in Singhal and Gupta, 2010; Sanderson and Nixon, 2015; Peacock et al., 2016). In this paper, we present and evaluate a 2D digital fracture network analysis method that is commonly use in structural geology, and through numerous case studies we demonstrate the potential wider uses of this

https://doi.org/10.5194/se-2019-184
Preprint. Discussion started: 10 December 2019




method for other users, for example geotechnical engineers, groundwater modellers and geomorphologists (Figure 1).

Fracture networks can be characterised in different dimensions using a number of approaches. 1D approaches include borehole fracture analysis and outcrop-based scanline surveys, typically represented by the number of fractures per unit length, i.e. frequency. 1D approaches are relatively rapid, but cannot directly constrain certain parameters such as fracture length and connectivity: if the fracture network is anisotropic (which is usually the case), the characterisation is biased by the orientation of the scanline or the borehole ('orientation bias'; Singhal and Gupta, 2010; Zeeb et al., 2013; Watkins et al. 2015b). 3D (really 2.5D) outcrop analysis using laser scanning provides a fuller analysis (e.g. Pless et al., 2015) but requires expensive equipment and is time-consuming in its processing. True 3D characterisation is possible using CT scanning, but is restricted to very small samples (Voorn et al. 2015). As a compromise, many studies employ a 2D approach. Normally, this uses some form of characterisation within a circular window of rock outcrop (Davies & Reynolds, 1996; Rohrbaugh et al. 2002; Watkins et al. 2015). Generally, for 2D analysis a scanline or window approach is taken, in the former fractures intersecting the line are recorded, whereas in the later fracture within the line area are recorded. Circular scanline methods are more rapid than full 2D circular window methods, have less length and orientation bias compared to 1D methods, but lack the full analysis of a complete 2D circular window approach. A circular scanline can be used to calculate proxies for fracture density and length based on the ratio of the types of trace intersection (Mauldon et al., 2001). Connectivity within two-dimensional fracture networks was parameterized by Manzocchi (2002), who characterised the different types of fracture intersections that can be used to characterise fluid flow properties.

A full 2D circular window characterisation in the field, using a circular 'chalk line' is a very time consuming method, and requires the outcrop to be fully accessible which may not be practical or safe. Building on previous work (Krabbendam and Bradwell, 2014; Pless et al., 2015; Watkins et al., 2015; Krabbendam et al. 2016; Healy et al., 2017) we present and develop a method for capturing a 2D fracture network from outcrop photographs as a digital (GIS) dataset. From this dataset, numerous key spatial relationships and parameters can be calculated. The only equipment needed are a decent digital camera, a measuring stick and GIS software (e.g. QGIS) for digitisation and analysis. This method can also be applied to georeferenced (orthorectified) aerial photos, hillshaded DTMs and satellite imagery for the characterisation of topographic lineaments. The method provides a relatively rapid and accessible way to generate accurate 2D fracture datasets and will be beneficial for a wide range of users including engineering geologists and hydrogeologists.

https://doi.org/10.5194/se-2019-184
Preprint. Discussion started: 10 December 2019


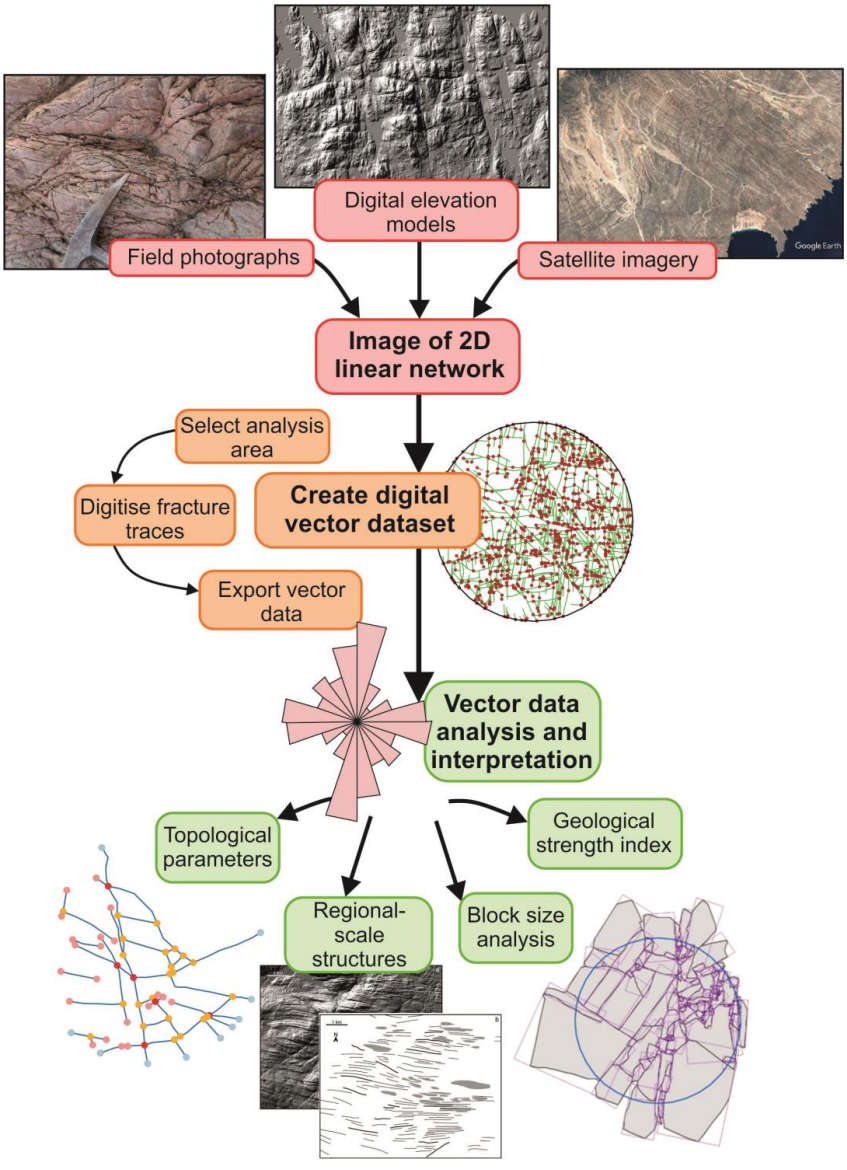


**Figure 1**: Flowchart providing an overview of the methodology used for digitising linear features, from preparing an image, digitising the features to output of data. Digital elevation model examples are taken from NEXTMap in Scotland (NEXTMap Britain elevation data from Intermap Technologies), and the satellite image of Oman example is taken from Google Earth ©.

https://doi.org/10.5194/se-2019-184
Preprint. Discussion started: 10 December 2019




## 2 Digital 2D fracture analysis method

The method in essence captures a set of digital traces (vectors) of a 2D linear feature network in a GIS project from a georeferenced image. Here, we use open source GIS software (QGIS), making the method accessible to all potential users. A number of open tools within QGIS can be used for more advanced analysis of the digitised fracture network.

### 2.1 Outcrop image preparation

The first step is to prepare a suitable photograph or image of the outcrop to be analysed. The image can be a photograph of a fracture network at outcrop of various scales from centimetres to 10s of metres. It is important that the fractures can be clearly identified in the photograph, and that not too much of the image is occupied by vegetation or broken ground (Figure 2a). It is important to include an accurate and clearly identifiable scale; a strip of plywood with duct tape works very well. However, in some dangerous outcrops (e.g. working quarries) this may be impractical and quarry machinery or other features of known dimensions may be used as a scale in the photograph. The photograph should be taken at right angles (or as much as possible) to the outcrop to minimise the issues created by a distortion of the image. The camera should have a focal length of 35mm (analogue 35 mm equivalent) or longer, to prevent further distortion. Horizontal outcrops should be photographed vertically to again minimise the distortion of the fractures. Mounting the camera on a stick is useful to increase the distance and capture a larger field of view (Figure 2b, c); or drones could also be used. For horizontal outcrops it is convenient to orient the measuring stick accurately to the north, using a compass (Figure 2c), this will allow corrections to be made for fracture orientations.

https://doi.org/10.5194/se-2019-184
Preprint. Discussion started: 10 December 2019


Solid Earth
Discussions
Open Access
EGU

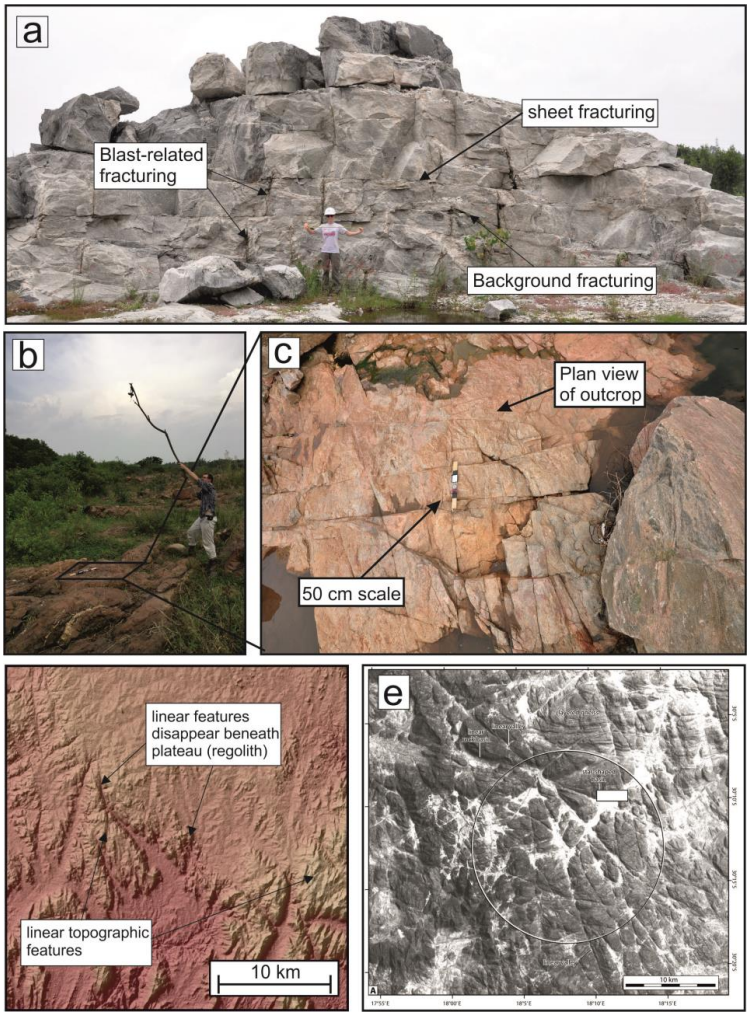


**Figure 2**: Examples of photographs and DEM images that can be used for digitising 2D linear features, including: (a-c) photographs of fracture networks of various scale from southern India and improvised methods for taking plan view photographs; (d) a DEM image from southern India of larger kilometre scale features that could also be digitised (SRTM digital elevation data); and (e) satellite images from Namibia showing a network of topographic lineaments (fracture zones) (adapted from Krabbendam and Bradwell, 2014).

https://doi.org/10.5194/se-2019-184
Preprint. Discussion started: 10 December 2019




105 **2.2 Using DEM images**

106 DEMs (Digital Elevation Models) (and their hill-shaded derivatives), satellite images and
107 (orthorectified) aerial photographs commonly show good topographic lineaments that likely represent
108 fracture zones, or master joints (Fig. 2d,e). Such imagery if georeferenced can be used directly
109 without further preparation. It should be noted however that aerial photographs, DEMs and satellite
110 images do not directly show fracture traces, rather they show the topographic expression of these.
111 Thus, fracture density is likely to be underestimated, because fractures with no topographic expression
112 will not be captured. Figure 2d is an example of a DEM image from southern India showing
113 kilometre-scale 2D topographic lineaments: in some parts lineaments are well developed, in other
114 parts fracture zones have no expression and presumably occur beneath a continuous layer of regolith.
115 Furthermore, such imagery is limited by the on-ground resolution, so that smaller-scale (smaller
116 aperture) fractures may not appear. For DEM-scale interpretations it is important to take a multi-data
117 type approach (e.g. geological maps and satellite images) to guide digitisation, similar to that of Pless
118 (2012).

119 **2.3 Georeferencing the images**

120 To aid robust georeferencing, the photograph needs to have a square of known size (e.g. 1 x 1 m)
121 embedded in it. This can be done by importing the photograph into a graphics software package (such
122 as Inkscape), and drawing a square based on the scale included in the original photograph (see Figure
123 3). The photograph with the embedded 1 x 1 m square is imported into a new GIS project file. The
124 GIS project file needs a projection in metres; we recommend a Mercator projection, (such as
125 EPSG:3857). Within the GIS project, a 'vector grid' is created, with a grid extent that is larger than
126 the imported photograph and with a vertical and horizontal spacing of 1.0. This will create a 1 m by 1
127 m vector grid (i.e. a fishnet grid) in the GIS project. Finally, georeference the square on the
128 photograph to a square on the fishnet grid, thus creating a georeferenced photograph within the GIS
129 project (Figure 3a).

https://doi.org/10.5194/se-2019-184
Preprint. Discussion started: 10 December 2019


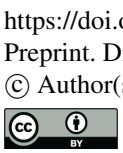

Solid Earth
Discussions
Open Access
EGU

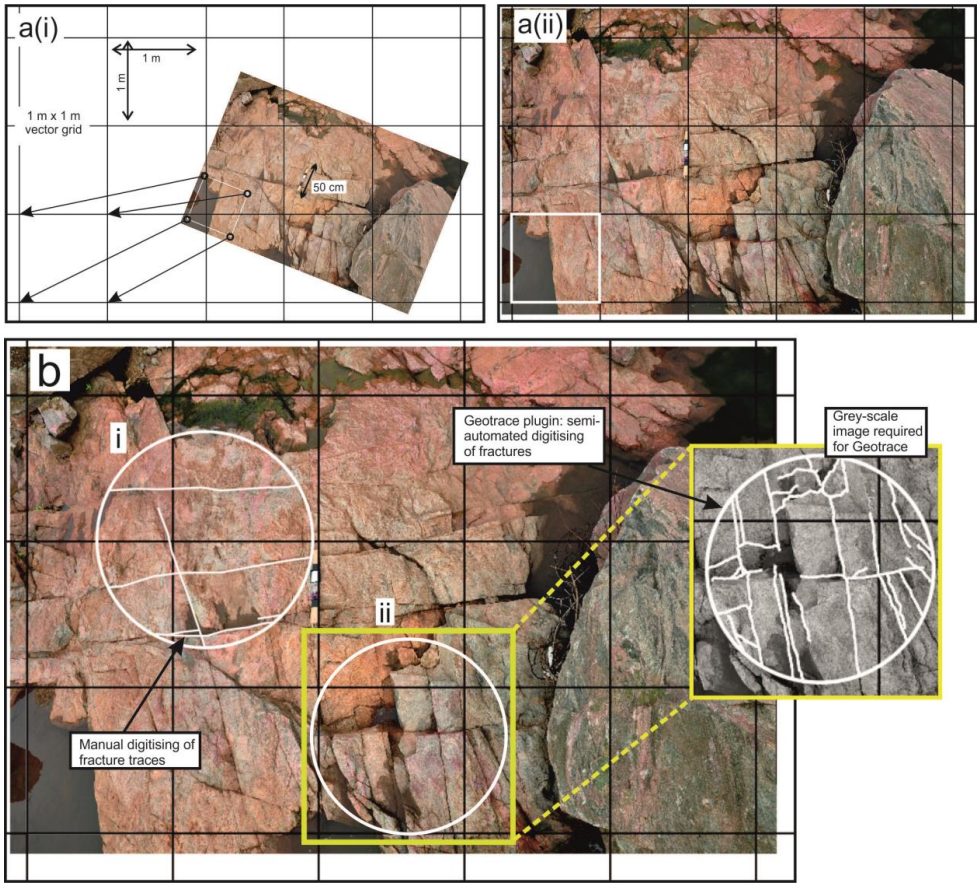


**Figure 3**: Images showing (a (i-ii)) how to georeference an image to a fishnet grid (black) from a square of a known scale (white); and (b) the tools available for digitising fractures in QGIS, including (i) a fully manual method; and (ii) a semi-automatic method such as Geotrace.

## 2.4 Data capture

### 2.4.1 Select analysis window

Different 2D lineament analysis windows can be used with this method including line scanlines, areal sampling and circular windows. For each of these methods a different shaped sample window is required. For this create a line or polygon shapefile and digitise the area that is to be analysed. An example is shown in Figure 3b as two circular windows, in white, digitised onto a photograph in GIS. It is important to create a different id number for each shape that includes details of the photograph or image that is being digitised.

https://doi.org/10.5194/se-2019-184
Preprint. Discussion started: 10 December 2019




### 2.4.2 Digitise linear features

This step aims to create a series of digital line traces from the georeferenced image. Create a new line shapefile in the GIS project to hold the linear trace data. The shapefile needs to include an id column in the attribute table so that the linear traces can be associated with a specific window and photograph. Two methods can be used to create digital traces of the linear features. Firstly, the individual features can be digitised manually in the GIS project, using the "add line features" tool. Alternatively, the plugin tool 'GeoTrace' can be used to semi-automate the digitising process. The GeoTrace plugin tool in QGIS allows one to click on the start and end of each fracture and GeoTrace creates a line vector between these points. For this method the photograph must be in grey scale, because the plugin follows the linear feature based on low raster values and requires a sharp contrast between the feature and the background. When digitising fracture traces it is important to only digitise in one orientation: if a feature has multiple orientations along its length then multiple lines should be digitised. Figure 3b is an example of both (i) manual digitisation and (ii) semi-automated digitisation with GeoTrace. In both the manual and semi-automated methods, it is important that connecting fractures are properly snapped against each other, and to the surrounding circular window.

## 2.5 Data output and further analysis

The final step is to generate basic parameters and calculate dimensions from the digital traces of the linear features. There are a number of different ways that the vector data can be analysed, which include: 1) using the field calculator in QGIS; 2) as an exported spreadsheet; or 3) using a programming language such as Python or ***R*** to make calculations directly from the shapefile.

Primary parameters can be calculated within the field calculator in the QGIS attribute table, including length and orientation of individual fracture traces. The area of the circular window can also be calculated in the attribute table using the field calculator. For further analysis, the attribute table containing the primary fracture data (length, orientation and reference to the circular window) needs to be exported as a spreadsheet, e.g. in CSV format. Fracture density ($D$) within the circular window can now be calculated using total length of fractures ($\Sigma L$) within the area of the circular window ($A$), following Singal & Gupta, (1999):

$$D = \Sigma L/A \quad (\text{in m}^{-1}) \qquad (1)$$

Fracture spacing (S) can be easily derived, as this is the reciprocal of fracture density, and is given by (Singal & Gupta, 1999):

$$S = A/\Sigma L \quad (\text{in m}). \qquad (2)$$

https://doi.org/10.5194/se-2019-184
Preprint. Discussion started: 10 December 2019




Other parameters, that can be derived from the digitised fracture network include the number and distribution of fracture intersections and block size. Fracture intersections (points) within the fracture network can be created as a separate point shapefile with the 'line intersection' tool.

The digitised fracture traces can also be used to derive block size parameters, using the 'polygonise' tool to convert the line vectors into polygons. As before, parameters such as area can be derived using the field calculator in the attribute table and exported as a spreadsheet.

## 3 Advantages and disadvantages

The digital method described here is not meant to replace field-based data gathering but used in conjunction, as it may be more suitable for different purposes. There are a number of advantages to using a digital method for gathering fracture data including: speed of gathering data, creating large datasets, flexibility in data gathering approach and consistency of data.

Gathering detailed 2D fracture network data in the field can often be a time consuming processes and therefore limits the amount of data that can be gathered during a field campaign. Using the digital methodology allows for fracture network data to be quickly gathered in the office, allowing for more data to be generated from an equivalent amount of time in the field. Field time can be used for detailed study of the outcrop to improve the interpretation of fractures in the office and to gather other key data such as aperture, fracture fill and 3D geometry's. The digital method allows for large, statistically significant datasets to be quickly gathered during a short field campaign. Collecting the data after fieldwork with a broader perspective provides an element of flexibility in terms of the selecting of outcrops for analysis, the type and shape of the sample window and the amount of the data gathered. Finally, the digital method has the potential to be used to improve the consistency and reliability of industry standards that involve fracture networks, such as rock mass strength estimates (Section 4.2) by reducing collector bias by standardising the data collection strategy.

For more evolved analysis of the fracture data the digital traces can be used in fracture analysis software packages such as FracPaQ (Healy et al., 2017), NetworkGT (Nymberg et al., 2018) and FraNEP (Zeeb et al., 2013). These programmes can be used for topological analysis such as deducing node types, and plotting fracture density heat maps illustrating density variations across a fracture zone.

A practical difficulty when analysing outcrops such as quarries, is to distinguish natural joints from those arising from blast damage. However, with experience based on field observations, blast damage can be separated from natural joints: on Figure 2a, some joints arising from blast damage are indicated, and can be easily distinguished from natural joints. Some basic initial observations in the field are beneficial for making such distinctions at a later stage; hence, it is recommended that the outcrops that are being analysed are always viewed in the field as well.

https://doi.org/10.5194/se-2019-184
Preprint. Discussion started: 10 December 2019


Solid Earth Discussions

There are limitations with capturing the data digitally. Firstly, the capturing of data in the field will always be more accurate in terms of seeing the full extent of fractures: for example, fractures may be obscured by vegetation making digitisation of traces more difficult than in the field (Andrews et al., 2019). Secondly, field observations of the character of individual fractures such as roughness, aperture and any secondary fills can be important observations made only in the field and useful when understanding rock mass strength or permeability. It is also possible, of course, to digitise the fracture network, and then return to the outcrop and augment the digital traces with further attribution that requires direct field observation (e.g. fracture aperture, fracture fill); portable PC tablets are ideal for this purpose. Image scale can also be an issue with this method, as smaller fractures can be harder to digitise from a wider perspective photograph, therefore it is important to acquire photographs that cover the appropriate scale of fractures, which will be dependent on the purpose of the study. Estimates of fracture permeability and percolation when using topology alone represent the maximum potential and does not account of closed fractures. Additional observations such as aperture and infilling are import for these types of studies.

## 4 Case studies

Below we present a number of case studies that include fracture analysis for groundwater modelling; quantifying rock mass properties for engineering geology; and block size distribution to understand sediment erodibility that help demonstrate the potential broader uses of the digital GIS-based analysis of fracture networks.

### 4.1 Understanding fracture connectivity and permeability, southern India

Characterisation of fracture networks is an important aspect of trying to understand local and regional-scale aquifer properties such as connectivity and permeability. This type of understanding is particularly relevant for groundwater studies in fractured ‘hard-rock’ aquifers, where fractures are the primary water stores and pathways (e.g. Stober and Bucher, 2007; Singal and Gupta 2010). An example is given here of the Peninsular Gneiss in the Cauvery Catchment in southern India. The groundwater properties of the Cauvery Catchment has been an area of ongoing research (Maréchal et al 2006, Perrin et al 2011) due to the spatial and temporal variability of groundwater availability and the impact that this has on local communities. Two contrasting basement fracture networks can be identified (Figure 4a-b): firstly, one massive gneiss with few fractures, dominated by a widely spaced ‘background jointing’ and sheeting joints close to the surface, and secondly ‘fracture zones’ that are characterised by a very dense fracture network.

https://doi.org/10.5194/se-2019-184
Preprint. Discussion started: 10 December 2019


Solid Earth
Discussions
Open Access
EGU

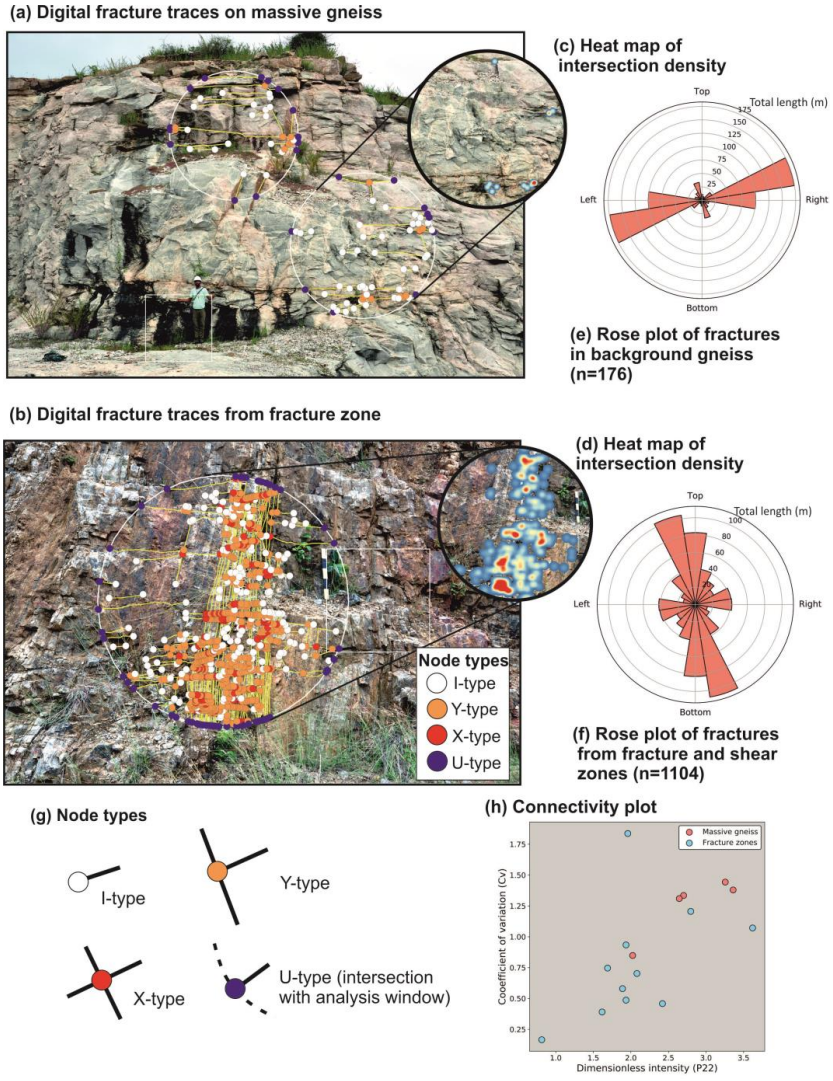


239

240 **Figure 4**: Fracture analysis from the Peninsular Gneiss, South India, including: field photographs with
241 digitised fracture branches and intersection types on (a) a massive gneiss example; and (b) from
242 a fracture zone; (c-d) heat maps illustrate variations in fracture intersection density (massive
243 gneiss: 0-5 nodes/m$^2$ and fracture zones: 0-18 nodes/m$^2$); (e-f) length-weighted rose plots
244 showing the variation in orientation of fractures traces in the background gneiss and fracture
245 zones; (g) a schematic illustration of the various types of fracture connections (as defined by
246 Manzocchi, 2002); (h) a plot of connections per line against dimensionless intensity (defined by
247 Sanderson and Nixon, 2015) to show variations in connectivity.

248

https://doi.org/10.5194/se-2019-184
Preprint. Discussion started: 10 December 2019


Rose plots show the variation in orientation of fractures in the two identified domains. In the massive gneiss the fractures are generally orientated sub-horizontally, with several short connecting vertical fractures. In contrast, fractures in the fracture zones are generally orientated sub-vertically with short connecting sub-horizontal fractures. The fracture density in the fracture zones is an order of magnitude higher than in the massive gneiss (Table 1). Using NetworkGT (Nymberg et al., 2018), the fracture branches and nodes (intersections and fracture trace end-points) were characterised based on the topology of the branch intersections (Sanderson and Nixon, 2015). The massive gneiss is dominated by I-type nodes, whereas the fracture zones predominantly contain a combination of Y- and X-type nodes (Figure 4a-b; for node types see Figure 4g) (Table 1). Heat maps of intersection clustering from the massive gneiss versus a fracture zone illustrate the higher connectivity of the fracture zones. To quantify the connectivity across the Cauvery catchment area the connections per line and dimensionless intensity (a proxy for intensity that reflects average fracture length) were calculated (following Sanderson and Nixon, 2015), (Table 1; Figure 4h). The connections per line, i.e the number of X- and Y-nodes per line, is an indication of the percolation potential of a fracture network (Sanderson and Nixon, 2018).The fracture zones have the highest connections per line and dimensionless intensity, suggesting they have the highest potential connectivity. In contrast, the background gneiss has the lowest connections per line and intensity suggesting a relatively low potential connectivity. The coefficient of variation (Cv) is calculated by dividing the standard deviation of the fracture spacing by the mean fracture spacing (Watkins et al., 2015a) and is used to quantify the how clustered a fracture network is (Table 1) (Oddling et al., 1999). The Cv ratios quantify the massive gneiss as generally having regularly-spaced fractures, while the fractures in the fracture zones are highly clustered (Table 1, Figure 4h).

At the near-surface, the Peninsular Gneiss has a bimodal fracture density distribution with areas of high fracture density that make up a relatively small proportion of the bedrock, and the majority of the crystalline basement comprises a low-density fracture pattern. Connectivity proxies, such as connections per line, indicate that the fracture zones have the highest potential permeability, whereas the permeability potential of the background gneiss is highly variable but still significantly lower.

In this case study, field time was limited and the digital method provided a quick and flexible way of gathering fracture network data. It was possible to survey the area that spans over 30,000 $km^2$ and then retrospectively select the most suitable sites for analysis. Key fracture parameters such as fracture length, orientation and density, which impacts on aquifer characteristics such as connectivity and permeability across the Peninsular Gneiss in the Cauvery River catchment, where then calculated and used to constrain local and regional-scale groundwater models.

https://doi.org/10.5194/se-2019-184
Preprint. Discussion started: 10 December 2019




284 **4.2 Rock mass strength estimates (Geological Strength Index)**

285 Structural discontinuities are an important control on the engineering behaviour of a rock mass
286 (Müller, 1974; Hoek 1994, Hoek & Brown 1997). Slopes, foundations and shallow underground
287 excavations in hard rock can be strongly be affected by the presence of discontinuities, for example,
288 the intersection of structural features can lead to falling and sliding of blocks or wedges from the
289 surface.
290
291 In the last decade, rock mass classification systems have been applied extensively in engineering
292 design and construction (Liu, 2007). The GSI (Geological Strength Index) system provides a
293 numerical representation of the overall geotechnical properties of a rock mass, which is estimated
294 using a standard matrix chart and field observations of (a) the 'blockiness' of a rock mass and (b) the
295 surface conditions of any discontinuities. The GSI Index is based upon an assessment of the lithology,
296 structure and condition of discontinuity surfaces in the rock mass and it is estimated from visual
297 examination of the rock mass exposed in surface excavations such as roadcuts, in tunnel faces and in
298 borehole core (Marinos and Hoek, 2000). Both the 'blockiness' and surface conditions, however, are
299 determined in a qualitative and descriptive manner, which is subjective and dependent on the
300 interpreter. Sönmez and Ulusay (1999; 2002) suggested that the 'blockiness' or Structure Rating can
301 be quantified by using the Volumetric Joint (fracture) Count (Jv, in $m^{-1}$). This parameter is defined as
302 the sum of the number of joints per meter for each joint set present (Sönmez & Ulusay, 1999), and can
303 be estimated by the following expression:
304
305 $$Jv = \frac{1}{S1} + \frac{1}{S2} + \cdots \frac{1}{Sn} \quad (3)$$
306
307 where *S* is the spacing of the joints in a set and *n* is the number of joint sets. The 2D fracture
308 digitisation method can clearly be applied to determine a more accurate representation of Jv from an
309 image.
310
311 The procedure for quantifying rock mass strength parameters in jointed rocks is illustrated using
312 massive and fractured gneiss exposures in India (Figure 4). Using the qualitative method (Hoek,
313 1983) the massive gneiss, with 'good' fracture surfaces, has a GSI index of 70-85 whereas the
314 fractured gneiss, with 'fair' fracture surfaces, has a GSI index of 30-45. To quantify this, the modified
315 GSI methodology (Sönmez & Ulusay (1999), see Figure 1) is used. In this example, the massive
316 gneiss has horizontal joint spacing of 0.81 m (J1) and vertical joint spacing of 6.19 m (J2). The
317 fractured gneiss has a horizontal joint spacing of 0.17 m (J1) and vertical joint spacing of 0.08 m (J2).
318 Thus, using equation 3, this gives a Jv value of 1.4 for the massive gneiss and 17.7 for the fractured
319 gneiss. Based on similar estimates of roughness (5), weathering (3) and infill (6) the fracture surface

https://doi.org/10.5194/se-2019-184
Preprint. Discussion started: 10 December 2019




condition rating (SCR) is 14. Finally, the GSI values calculated are *ca*. 76 for the massive gneiss and only *ca*. 44 for the fractured gneiss, demonstrating an accurate representation of the rock mass strength differences of the massive and fractured gneiss.

When determining rock mass strength properties the digital method can provide a fast, accurate and consistent result. Understanding rock mass strength properties is relevant for both academic and industry users, in both cases, available field time can often be limited. In addition, particularly in industry there is likely to be multiple interpreters making rock mass strength estimates, and therefore this method can help improve consistency in the results by undertaking analysis digitally.

### 4.3 Block size and rock erodibility, Southern Scotland

Fracturing is a significant factor in the preconditioning of rock masses for erosion at the Earth's surface (e.g. Roy et al., 2016; Clarke and Burbank, 2010). As well as influencing the volume of material available for mobilisation and transport, fracturing of bedrock is a key control on the clast size distribution of eroded material entering geomorphic systems from hillslopes, particularly in upland landscapes (e.g. Sklar et al. 2016).

The 2D fracture digitisation method is here used to assess the spatial distribution of block-size and fracture intensity of metasandstone of low metamorphic grade in the Southern Uplands, southern Scotland. Block density can be expressed as blocks per square metre, which is easily derived from a polygonised set of fracture traces. It should be noted that whether this 2D block size measure is representative for the true 3D block size depends on the anisotropy of the fracture system and the average block shape. Despite consistent bedrock type (metasandstone) across the study area, the anisotropic fracture pattern gives rise to strong variations in block-size as shown by variation in the number of blocks sampled per unit measuring area from <50 to >1000 blocks per $m^2$ (Figure 5). This data can help to quantify key controls on the influence of facture intensity on block size, which may be used to inform modelling erosion and sediment movement within landscapes.

For this study, a large amount of fracture and block data was required from several outcrops, and the digital method provided an accurate and efficient way for gathering large amounts of fracture and block size data. Due to the requirements of the study, photographs were taken close to the outcrop to improve the accuracy of digitisation (Figure 5a), resulting in a large and accurate dataset.

https://doi.org/10.5194/se-2019-184
Preprint. Discussion started: 10 December 2019




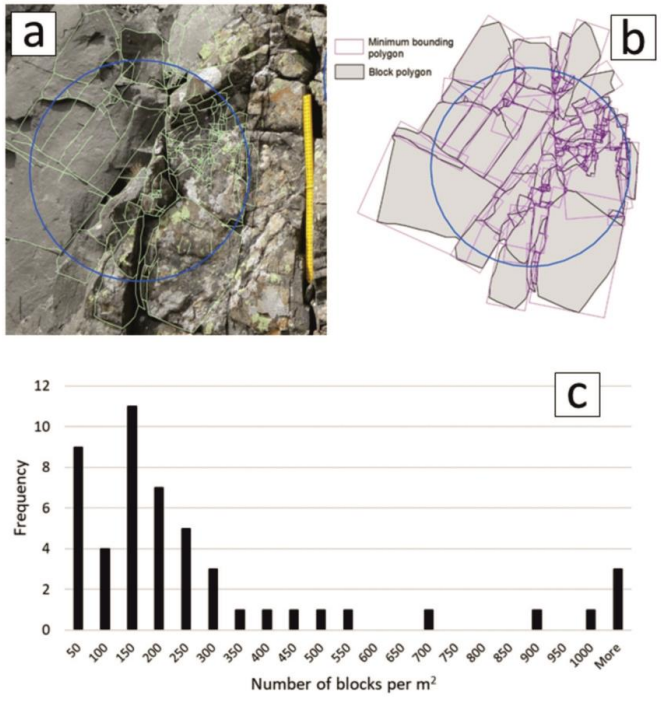


**Figure 5.** Derivation of block-size metrics for Wacke sandstone in the Southern Uplands of Scotland. Field photograph of sandstone outcrop with fracture delineation (a), polygons for blocks sampled by the circular window (b), number of blocks sampled per $m^2$ for dataset of 50 measuring sites from the study area.

## 5 Conclusions

The aim of this paper is to review and evaluate the methodology for digitising 2D fracture networks in GIS, and make it more accessible to a broader range of users in both academia and industry. We present a breakdown of the key steps in the methodology, which provides an understanding of how to avoid error and improve the accuracy of the final dataset.

The digital method can be used to interpret traces of 2D linear features of a wide variety of scales from the micro-scale to the kilometre scale, including lineations or mineral cleavages from a photomicrograph, fractures at outcrop scale to regional-scale structural lineaments that are visible on aerial photographs or DEMs.

An important aspect of applied geosciences, such as hydrogeology and geotechnical engineering is the accurate parameterisation of fracture networks in bedrock. The methodology that is commonly used is

https://doi.org/10.5194/se-2019-184
Preprint. Discussion started: 10 December 2019




a qualitative description and can be time consuming. The digital 2D fracture trace capture method is an accurate and rapid way of quantifying 2D linear networks such as fracture zones using open access software packages. It offers a robust, cost-effective methodology that can used in academy and industry to gather accurate 2D fracture network data.

**Acknowledgements**

The research underlying this paper was carried out jointly under the UPSCAPE project of the Newton-Bhabha programme "Sustaining Water Resources for Food, Energy and Ecosystem Services", funded by the UK Natural Environment Research Council (NERC-UKRI) and the India Ministry of Earth Sciences (MoES), grant number NE/N016270/1; and by the British Geological Survey NC-ODA grant NE/R000069/1: *Geoscience for Sustainable Futures.* British Geological Survey (BGS-UKRI) publish with the permission of the Director of BGS. The views and opinions expressed in this paper are those of the authors alone. Martin Gillespie is thanked for helpful comments on the manuscript.

https://doi.org/10.5194/se-2019-184
Preprint. Discussion started: 10 December 2019




## References

Andrews, B. J., Roberts, J. J., Shipton, Z. K., Bigi, S., Tartarello, M. C., and Johnson, G.: How do we see fractures? Quantifying subjective bias in fracture data collection, Solid Earth, 10, 487-516, 2019.

Bandpey, A. K., Shahriar, K., Sharifzadeh, M., and Marefvand, P.: Comparison of methods for calculating geometrical characteristics of discontinuities in a cavern of the Rudbar Lorestan power plant, Bulletin of Engineering Geology and the Environment, 1-21, 2017.

Barton, N., Lien, R., and Lunde, J.: Engineering classification of rock masses for the design of tunnel support, Rock mechanics, 6, 189-236, 1974.

Bieniawski, Z. T.: Rock mechanics design in mining and tunnelling, Monograph, 1984.

Bieniawski, Z. T., and Bieniawski, Z.: Engineering rock mass classifications: a complete manual for engineers and geologists in mining, civil, and petroleum engineering, John Wiley & Sons, 1989.

Clarke, B. A., and Burbank, D. W.: Bedrock fracturing, threshold hillslopes, and limits to the magnitude of bedrock landslides, Earth and Planetary Science Letters, 297, 577-586, 2010.

Dühnforth, M., Anderson, R. S., Ward, D., and Stock, G. M.: Bedrock fracture control of glacial erosion processes and rates, Geology, 38, 423-426, 2010.

Follin, S., Hartley, L., Rhén, I., Jackson, P., Joyce, S., Roberts, D., and Swift, B.: A methodology to constrain the parameters of a hydrogeological discrete fracture network model for sparsely fractured crystalline rock, exemplified by data from the proposed high-level nuclear waste repository site at Forsmark, Sweden, Hydrogeology Journal, 22, 313-331, 2014.

Guihéneuf, N., Boisson, A., Bour, O., Dewandel, B., Perrin, J., Dausse, A., Viossanges, M., Chandra, S., Ahmed, S., and Maréchal, J.: Groundwater flows in weathered crystalline rocks: Impact of piezometric variations and depth-dependent fracture connectivity, Journal of Hydrology, 511, 320-334, 2014.

Hardebol, N., and Bertotti, G.: DigiFract: A software and data model implementation for flexible acquisition and processing of fracture data from outcrops, Computers & Geosciences, 54, 326-336, 2013.

Healy, D., Rizzo, R. E., Cornwell, D. G., Farrell, N. J., Watkins, H., Timms, N. E., Gomez-Rivas, E., and Smith, M.: FracPaQ: A MATLAB™ toolbox for the quantification of fracture patterns, Journal of Structural Geology, 95, 1-16, 2017.

Hoek, E.: Strength of jointed rock masses, Geotechnique, 33, 187-223, 1983.

Hoek, E., and Brown, E. T.: Practical estimates of rock mass strength, International journal of rock mechanics and mining sciences, 34, 1165-1186, 1997.

https://doi.org/10.5194/se-2019-184
Preprint. Discussion started: 10 December 2019


429 Hong, K., Han, E., and Kang, K.: Determination of geological strength index of jointed rock mass
430 based on image processing, Journal of Rock Mechanics and Geotechnical Engineering, 9, 702-
431 708, 2017.
432 Hooyer, T. S., Cohen, D., and Iverson, N. R.: Control of glacial quarrying by bedrock joints,
433 Geomorphology, 153, 91-101, 2012.
434 Krabbendam, M., and Glasser, N. F.: Glacial erosion and bedrock properties in NW Scotland:
435 abrasion and plucking, hardness and joint spacing, Geomorphology, 130, 374-383, 2011.
436 Krabbendam, M., and Bradwell, T.: Quaternary evolution of glaciated gneiss terrains: pre-glacial
437 weathering vs. glacial erosion, Quaternary Science Reviews, 95, 20-42, 2014.
438 Krabbendam, M., Eyles, N., Putkinen, N., Bradwell, T., and Arbelaez-Moreno, L.: Streamlined hard
439 beds formed by palaeo-ice streams: A review, Sedimentary Geology, 338, 24-50, 2016.
440 Laubach, S. E., Lamarche, J., Gauthier, B. D., Dunne, W. M., and Sanderson, D. J.: Spatial
441 arrangement of faults and opening-mode fractures, Journal of Structural Geology, 108, 2-15,
442 2018.
443 Liu, Y.-C., and Chen, C.-S.: A new approach for application of rock mass classification on rock slope
444 stability assessment, Engineering geology, 89, 129-143, 2007.
445 Mahé, S., Gasc-Barbier, M., and Soliva, R.: Joint set intensity estimation: comparison between
446 investigation modes, Bulletin of Engineering Geology and the Environment, 74, 171-180, 2015.
447 Mäkel, G.: The modelling of fractured reservoirs: Constraints and potential for fracture network
448 geometry and hydraulics analysis, Geological Society, London, Special Publications, 292, 375-
449 403, 2007.
450 Manzocchi, T.: The connectivity of two-dimensional networks of spatially correlated fractures, Water
451 Resources Research, 38, 1-1-1-20, 2002.
452 Maréchal, J.-C., Dewandel, B., Ahmed, S., Galeazzi, L., and Zaidi, F. K.: Combined estimation of
453 specific yield and natural recharge in a semi-arid groundwater basin with irrigated agriculture,
454 Journal of Hydrology, 329, 281-293, 2006.
455 Marinos, P., and Hoek, E.: GSI: a geologically friendly tool for rock mass strength estimation, ISRM
456 international symposium, 2000,
457 Mauldon, M., Dunne, W., and Rohrbaugh Jr, M.: Circular scanlines and circular windows: new tools
458 for characterizing the geometry of fracture traces, Journal of Structural Geology, 23, 247-258,
459 2001.
460 Müller, L.: Rock mechanics, Springer, 1974.
461 Nyberg, B., Nixon, C. W., and Sanderson, D. J.: NetworkGT: A GIS tool for geometric and
462 topological analysis of two-dimensional fracture networks, Geosphere, 14, 1618-1634, 2018.
463 Odling, N., Gillespie, P., Bourgine, B., Castaing, C., Chiles, J., Christensen, N., Fillion, E., Genter,
464 A., Olsen, C., and Thrane, L.: Variations in fracture system geometry and their implications for
465 fluid flow in fractures hydrocarbon reservoirs, Petroleum Geoscience, 5, 373-384, 1999.

https://doi.org/10.5194/se-2019-184
Preprint. Discussion started: 10 December 2019




466 Park, H.-J., West, T. R., and Woo, I.: Probabilistic analysis of rock slope stability and random
467 properties of discontinuity parameters, Interstate Highway 40, Western North Carolina, USA,
468 Engineering Geology, 79, 230-250, 2005.
469 Peacock, D., Nixon, C., Rotevatn, A., Sanderson, D., and Zuluaga, L.: Glossary of fault and other
470 fracture networks, Journal of Structural Geology, 92, 12-29, 2016.
471 Peacock, D., Dimmen, V., Rotevatn, A., and Sanderson, D.: A broader classification of damage zones,
472 Journal of Structural Geology, 102, 179-192, 2017.
473 Peacock, D., Sanderson, D., and Rotevatn, A.: Relationships between fractures, Journal of Structural
474 Geology, 106, 41-53, 2018.
475 Perrin, J., Ahmed, S., and Hunkeler, D.: The effects of geological heterogeneities and piezometric
476 fluctuations on groundwater flow and chemistry in a hard-rock aquifer, southern India,
477 Hydrogeology Journal, 19, 1189, 2011.
478 PLESS, J.: Characterising fractured basement using the Lewisian Gneiss Complex, NW Scotland:
479 implications for fracture systems in the Clair Field basement, Durham University, 2012.
480 Pless, J., McCaffrey, K., Jones, R., Holdsworth, R., Conway, A., and Krabbendam, M.: 3D
481 characterization of fracture systems using terrestrial laser scanning: An example from the
482 Lewisian basement of NW Scotland, Geological Society, London, Special Publications, 421,
483 125-141, 2015.
484 Procter, A., and Sanderson, D. J.: Spatial and layer-controlled variability in fracture networks, Journal
485 of Structural Geology, 108, 52-65, 2018.
486 Ren, F., Ma, G., Fan, L., Wang, Y., and Zhu, H.: Equivalent discrete fracture networks for modelling
487 fluid flow in highly fractured rock mass, Engineering geology, 229, 21-30, 2017.
488 Rizzo, R. E., Healy, D., and De Siena, L.: Benefits of maximum likelihood estimators for fracture
489 attribute analysis: Implications for permeability and up-scaling, Journal of Structural Geology,
490 95, 17-31, 2017.
491 Roy, S., Tucker, G., Koons, P., Smith, S., and Upton, P.: A fault runs through it: Modeling the
492 influence of rock strength and grain-size distribution in a fault-damaged landscape, Journal of
493 Geophysical Research: Earth Surface, 121, 1911-1930, 2016.
494 Sanderson, D. J., and Nixon, C. W.: The use of topology in fracture network characterization, Journal
495 of Structural Geology, 72, 55-66, 2015.
496 Sanderson, D. J., and Nixon, C. W.: Topology, connectivity and percolation in fracture networks,
497 Journal of Structural Geology, 115, 167-177, 2018.
498 Selby, M. J.: Hillslope materials and processes, Hillslope materials and processes., 1982.
499 Singhal, B. B. S., and Gupta, R. P.: Applied hydrogeology of fractured rocks, Springer Science &
500 Business Media, 2010.

https://doi.org/10.5194/se-2019-184
Preprint. Discussion started: 10 December 2019




Sklar, L. S., Riebe, C. S., Marshall, J. A., Genetti, J., Leclere, S., Lukens, C. L., and Merces, V.: The problem of predicting the size distribution of sediment supplied by hillslopes to rivers, Geomorphology, 277, 31-49, 2017.

Sonmez, H., and Ulusay, R.: Modifications to the geological strength index (GSI) and their applicability to stability of slopes, International Journal of Rock Mechanics and Mining Sciences, 36, 743-760, 1999.

Sonmez, H., and Ulusay, R.: A discussion on the Hoek-Brown failure criterion and suggested modifications to the criterion verified by slope stability case studies, Yerbilimleri, 26, 77-99, 2002.

Sturzenegger, M., Sartori, M., Jaboyedoff, M., and Stead, D.: Regional deterministic characterization of fracture networks and its application to GIS-based rock fall risk assessment, Engineering geology, 94, 201-214, 2007.

Sturzenegger, M., Stead, D., and Elmo, D.: Terrestrial remote sensing-based estimation of mean trace length, trace intensity and block size/shape, Engineering Geology, 119, 96-111, 2011.

Thiele, S. T., Grose, L., Samsu, A., Micklethwaite, S., Vollgger, S. A., and Cruden, A. R.: Rapid, semi-automatic fracture and contact mapping for point clouds, images and geophysical data, Solid Earth, 8, 1241, 2017.

Watkins, H., Bond, C. E., Healy, D., and Butler, R. W.: Appraisal of fracture sampling methods and a new workflow to characterise heterogeneous fracture networks at outcrop, Journal of Structural Geology, 72, 67-82, 2015.

Watkins, H., Butler, R. W., Bond, C. E., and Healy, D.: Influence of structural position on fracture networks in the Torridon Group, Achnashellach fold and thrust belt, NW Scotland, Journal of Structural Geology, 74, 64-80, 2015.

Zeeb, C., Gomez-Rivas, E., Bons, P. D., and Blum, P.: Evaluation of sampling methods for fracture network characterization using outcrops, AAPG bulletin, 97, 1545-1566, 2013.

Zeeb, C., Gomez-Rivas, E., Bons, P. D., Virgo, S., and Blum, P.: Fracture network evaluation program (FraNEP): A software for analyzing 2D fracture trace-line maps, Computers & geosciences, 60, 11-22, 2013.

Zhan, J., Xu, P., Chen, J., Wang, Q., Zhang, W., and Han, X.: Comprehensive characterization and clustering of orientation data: A case study from the Songta dam site, China, Engineering geology, 225, 3-18, 2017.

https://doi.org/10.5194/se-2019-184
Preprint. Discussion started: 10 December 2019




536

537

538

539

540

541

542

543

544

| Rock type | Area(m2) | Mean length (m) | 2D density (m-2) | I | U | X | Y | Dimensionless intensity | Connections per line | Coefficient of variation (Cv) |
|---|---|---|---|---|---|---|---|---|---|---|
| Shear zone | 4.6 | 0.2 | 17.8 | 157.0 | 61.0 | 121.0 | 517.0 | 3.3 | 3.8 | 1.4 |
| Bangalore-region gneiss | 15.0 | 0.6 | 1.4 | 41.0 | 10.0 | 1.0 | 11.0 | 0.8 | 0.9 | 0.2 |
| Bangalore-region gneiss | 11.9 | 1.0 | 1.9 | 19.0 | 15.0 | 0.0 | 10.0 | 1.9 | 1.4 | 0.6 |
| Bangalore fracture zone | 26.8 | 0.5 | 3.9 | 136.0 | 32.0 | 18.0 | 157.0 | 2.0 | 2.4 | 0.8 |
| Bangalore fracture zone | 8.5 | 0.3 | 8.8 | 130.0 | 40.0 | 38.0 | 204.0 | 2.7 | 2.9 | 1.3 |
| Mysore-region gneiss | 137.8 | 2.9 | 0.7 | 21.0 | 10.0 | 6.0 | 23.0 | 1.9 | 2.6 | 0.9 |
| Shear zone | 45.2 | 0.9 | 3.9 | 139.0 | 38.0 | 45.0 | 174.0 | 3.4 | 2.8 | 1.4 |
| Shear zone | 38.5 | 1.7 | 1.6 | 139.0 | 38.0 | 45.0 | 174.0 | 2.6 | 2.8 | 1.3 |
| Mysore-region gneiss | 81.6 | 2.6 | 1.1 | 23.0 | 16.0 | 6.0 | 25.0 | 2.8 | 2.6 | 1.2 |
| Bangalore-region gneiss | 359.4 | 11.9 | 0.2 | 5.0 | 4.0 | 1.0 | 1.0 | 2.0 | 1.3 | 1.8 |
| Bangalore-region gneiss | 31.1 | 5.3 | 0.7 | 3.0 | 5.0 | 0.0 | 0.0 | 3.6 | 0.0 | 1.1 |
| Bangalore-region gneiss | 9.2 | 1.5 | 1.4 | 4.0 | 6.0 | 0.0 | 6.0 | 2.1 | 2.4 | 0.7 |
| Bangalore-region gneiss | 13.3 | 2.1 | 0.9 | 2.0 | 8.0 | 0.0 | 2.0 | 1.9 | 2.0 | 0.5 |
| Bangalore-region gneiss | 10.5 | 1.9 | 0.9 | 2.0 | 5.0 | 2.0 | 1.0 | 1.7 | 4.0 | 0.7 |
| Bangalore-region gneiss | 119.6 | 2.1 | 0.8 | 41.0 | 12.0 | 4.0 | 27.0 | 1.6 | 1.8 | 0.4 |
| Bangalore-region gneiss | 95.4 | 2.3 | 1.0 | 29.0 | 19.0 | 5.0 | 30.0 | 2.4 | 2.4 | 0.5 |

545

546 **Table 1.** An overview of key fracture network data from the Peninsular Gneiss from Cauvery River
547 Catchment in southern India.

548

549

550

551